

# Dark Matter in the Constrained NMSSM

C. Hugonie<sup>1</sup>, G. Bélanger<sup>2</sup>, A. Pukhov<sup>3</sup>

1) *Laboratoire Physique Théorique et Astroparticules*  
*Unité mixte de Recherche – CNRS – UMR5207*  
*Université de Montpellier II, F-34095 Montpellier, France*  
2) *Laboratoire d’Annecy-le-Vieux de Physique Théorique*  
*Unité mixte de Recherche – CNRS – UMR5108*  
*Université de Savoie, F-74941 Annecy-le-Vieux, France*  
3) *Skobeltsyn Institute of Nuclear Physics*  
*Moscow State University, 119992 Moscow, Russia*

February 27, 2019

## Abstract

We explore the parameter space of the Constrained Next-to-Minimal Supersymmetric Standard Model with GUT scale boundary conditions (CNMSSM), and find regions where the relic density of the lightest neutralino is compatible with the WMAP measurement. We emphasize differences with the MSSM: cases where annihilation of the LSP occurs via a Higgs resonance at low values of  $\tan\beta$  and cases where the LSP has a large singlino component. The particle spectrum as well as theoretical and collider constraints are calculated with `NMSSMTools`. All neutralino annihilation and coannihilation processes are then computed with `micrOMEGAs`, taking into account higher order corrections to the Higgs sector.

## 1 Introduction

One of the attractive features of supersymmetric (SUSY) extensions of the Standard Model (SM) with conserved R-parity, is the presence of a good Dark Matter (DM) candidate, the lightest SUSY particle (LSP). Over the years, numerous studies have examined the constraints on the parameter space of the constrained minimal supersymmetric standard model (CMSSM) including that originating from the precise measurement of the DM relic density, the WMAP result is  $.094 < \Omega h^2 < .129$  at  $2\sigma$  [1]. All concluded that the CMSSM could in some region of parameter space provide a satisfactory DM candidate [2–9]. The MSSM, or its constrained version, however face a naturalness problem – the so-called  $\mu$  problem. The NMSSM is the simplest extension of the MSSM that solves this problem elegantly via the introduction of a gauge singlet superfield,  $S$ . The effective  $\mu$  parameter term is determined by the vev of this singlet field, which is naturally of EW scale [10–18].

The NMSSM contains an extra scalar and pseudoscalar states in the Higgs sector as well as an additional neutralino, the singlino. Owing both to modifications in the Higgs sector and the neutralino sector, the DM properties can differ from those of the MSSM [19–24]. In particular a LSP with a large singlino component has different annihilation properties than the bino LSP that is in general found in the CMSSM. It is even possible to have a very light singlino LSP if accompanied by a very light scalar. Even when the LSP has no singlino component, the more elaborate Higgs sector of the model provides additional channels for

rapid annihilation through Higgs exchange. This can have implications for direct and indirect detection rates [24–27].

The constrained version of the NMSSM (CNMSSM) with parameters defined at the GUT scale has not been explored yet. This is the purpose of this paper. In this first analysis we emphasize the differences with the CMSSM predictions as concerns the neutralino properties and its annihilation. We will therefore concentrate on regions of parameter space where the LSP has some singlino component as well as regions where the spectrum is such that annihilation can take place near a Higgs resonance. In the former case, we will see that coannihilation processes, with staus or other neutralinos play a crucial role. Of course, in large regions of parameter space we expect to recover features of the CMSSM with a LSP that is mostly bino and can only annihilate efficiently near a Higgs resonance or coannihilate with light sleptons. In this case the only difference with the CMSSM will be additional allowed parameter space due to relaxed constraints from LEP on the Higgs sector.

To evaluate the supersymmetric spectrum we use the NMSPEC program from the `NMSSMTools` package [28]. Using renormalization group equations (RGEs) and starting from GUT scale parameters, this code computes the Higgs spectrum including higher order corrections as well as the masses of sparticles at one-loop. It also checks all the available collider constraints as well as various theoretical constraints. For the computation of the relic density of DM we rely on `micrOMEGAs` [29] which is included in `NMSSMTools`.

The paper is organized as follows: in sec. 2 we briefly describe the model. In sec. 3 we discuss the main channels for annihilation. In sec. 4 we present typical case studies. Conclusions follow in sec. 5.

## 2 The CNMSSM

In the present paper we discuss the simplest version of the NMSSM with a scale invariant superpotential

$$W = \lambda S H_u H_d + \frac{\kappa}{3} S^3 + (\text{Yukawa couplings}), \quad (2.1)$$

which is the only supersymmetric extension of the Standard Model where the weak scale originates from the soft SUSY breaking scale only, i.e. where no supersymmetric dimensionful parameters as  $\mu$  are present in the superpotential <sup>1</sup>.

Constraining the parameters of the NMSSM by imposing universality at the GUT scale is not as direct as in the MSSM. In the CMSSM, the free parameters are the universal GUT scale soft terms  $A_0$ ,  $m_0$  and  $M_{1/2}$ . In addition,  $M_Z$  and  $\tan\beta$  (at the weak scale) are used as inputs, and the two minimization equations of the Higgs potential w.r.t. the two real Higgs vevs  $h_u$  and  $h_d$  are used to compute  $\mu$  and  $B$  in terms of the other parameters (this leaves the sign of  $\mu$  as a free parameter). Both  $\mu$  and  $B$  have only a small effect on the RGEs of the other parameters (via threshold effects from particles whose masses depend on  $\mu$  and/or  $B$ ). In numerical codes, this is usually solved by an iterative procedure.

At first sight, an application of this procedure to the NMSSM is not obvious: both  $\mu$  and  $B$  are no longer independent parameters and one has to cope with three coupled mini-

---

<sup>1</sup>Note that the nearly minimal supersymmetric standard model (nMSSM) has in addition a tadpole term for the singlet in the superpotential and/or in the soft scalar potential [30–32]. The DM properties within this model, with special attention to the possibility of generating the baryon asymmetry of the universe have been analysed in refs. [33–36].

mization equations w.r.t.  $h_u$ ,  $h_d$  and  $s$ . However, one can still define effective ( $s$  dependent) parameters:

$$\mu = \lambda s, \quad \nu = \kappa s, \quad B = A_\lambda + \nu. \quad (2.2)$$

(In the following, we will always use  $\nu$  rather than  $\kappa$ ). The minimization equations w.r.t.  $h_u$  and  $h_d$  can then be solved for  $\mu$  and  $B$ , as in the MSSM, in terms of the other parameters (incl.  $M_Z$  and  $\tan\beta$ ). From  $\mu$  and  $B$  one can deduce (for  $\lambda$  and  $A_\lambda$  given) both  $s$  and  $\kappa$ . Finally, from the minimization equation w.r.t.  $s$ , one can easily obtain the soft singlet mass  $m_S^2$  in terms of all other parameters. At tree level, the minimization equations read:

$$\begin{aligned} \mu^2 &= \frac{m_{H_d}^2 - m_{H_u}^2 \tan\beta^2}{\tan\beta^2 - 1} - \frac{1}{2}M_Z^2, \\ B &= \frac{\sin 2\beta}{2\mu} (m_{H_u}^2 + m_{H_d}^2 + 2\mu^2 + \lambda^2(h_u^2 + h_d^2)), \\ m_S^2 &= \lambda^2 \frac{h_u h_d}{\mu} (A_\lambda + 2\nu) - \nu(A_\kappa + 2\nu) - \lambda^2(h_u^2 + h_d^2). \end{aligned} \quad (2.3)$$

The radiative corrections to the scalar potential show a weak dependence on  $s$ ,  $\kappa$  and  $m_S^2$  which can be included in the minimization equations. These become non-linear in the parameters to solve for and have therefore to be solved iteratively. The derived parameters  $\kappa$  and  $m_S^2$  affect the RGEs of the other parameters not only through threshold effects around  $M_{\text{susy}}$ , but also through the  $\beta$  functions. However, the numerical impact is relatively small such that an iterative procedure converges quite rapidly again.

As  $m_S^2$  is an output, it is difficult to find parameters such that  $m_S^2$  assumes the same value as the Higgs doublet (or other scalar) soft masses squared at the GUT scale. On the other hand, the mechanism for the generation of soft SUSY breaking terms could easily treat the singlet differently from the other non-singlet matter multiplets. Hence, we assume the following free parameters for the CNMSSM:

- $\tan\beta$ ,  $\text{sign}(\mu)$  at the weak scale;
- $\lambda$  at the SUSY scale;
- universal soft terms  $M_{1/2}$ ,  $m_0$  and  $A_0$  at the GUT scale. Exceptions are:
  - $m_S^2$  at the GUT scale which is an output, as described above;
  - the trilinear coupling  $A_\kappa$  at the GUT scale. The reason for this is twofold: first,  $A_\kappa = A_0$  usually leads to negative mass squared in the Higgs sector. Second, if an underlying mechanism for the generation of the soft SUSY breaking terms treats the singlet differently from the other matter fields (as it is already assumed for  $m_S^2$ ), this will also affect the coupling  $A_\kappa$  which involves the singlet only.

Not all choices of parameters are allowed in the CNMSSM. Some lead to negative mass squared for scalar fields (Higgs or sfermions), others to Landau poles below the GUT scale for the dimensionless couplings. The `NMSSMTools` package also includes all the available experimental constraints from LEP and Tevatron on sparticle and Higgs searches (for details on the exclusion channels see refs. [28, 37]). It is the aim of this paper to find out which regions in the parameter space of the CNMSSM can fulfill all the theoretical and experimental

tests and at the same time provide the correct amount of DM. In sec. 4, we will present quantitative results, but let us first have a qualitative approach here.

In order to do this, it is helpful to have a look at the symmetric  $3 \times 3$  CP even Higgs mass matrix at tree level:

$$\mathcal{M}_S^2 = \begin{bmatrix} g^2 h_u^2 + \mu B \frac{h_d}{h_u} & (2\lambda^2 - g^2) h_u h_d - \mu B & 2\lambda h_u \mu - \lambda h_d (A_\lambda + 2\nu) \\ & g^2 h_d^2 + \mu B \frac{h_u}{h_d} & 2\lambda h_d \mu - \lambda h_u (A_\lambda + 2\nu) \\ & & \lambda^2 A_\lambda \frac{h_u h_d}{\mu} + \nu (A_\kappa + 4\nu) \end{bmatrix}. \quad (2.4)$$

To a good approximation, the  $2 \times 2$  doublet subsector is diagonalized by the angle  $\beta$  which gives a light eigenstate  $h$  with mass

$$m_h = \left( \cos^2 2\beta + \frac{\lambda^2}{g^2} \sin^2 2\beta \right) M_Z^2 \quad (2.5)$$

and a heavy eigenstate  $H$  with a mass  $m_H \sim m_A$  close to the MSSM-like CP odd state (the larger  $m_A$ , the better this approximation). In the NMSSM, one can define  $m_A^2$  as the diagonal doublet term in the CP odd  $2 \times 2$  mass matrix after the Goldstone mode has been dropped. At tree level, it has the same expression as in the MSSM:

$$m_A^2 = \frac{2\mu B}{\sin 2\beta}. \quad (2.6)$$

It is already well known that large values of  $\lambda$  are not allowed in the NMSSM as they would imply a Landau pole below the GUT scale. This leads to an upper bound on  $\lambda \lesssim .7$  which depends on  $\tan\beta$ . Values of  $\lambda \gtrsim .1$  are not always allowed in the CNMSSM: on the one hand  $\lambda$  increases the mass of the light state  $h$ . This increase is relevant, however, only for small  $\tan\beta$ . On the other hand,  $\lambda$  induces mixings between the doublet and the singlet states. Since the singlet state is typically heavier than  $\sim 100$  GeV, this mixing reduces the mass of the lightest eigenstate  $h$  which will then often violate bounds from LEP. In order to maximize the mass of the lightest CP even mass eigenstate, this singlet-doublet mixing has to vanish (as described in [38]), which implies a relation between  $\mu$ ,  $\nu$ ,  $A_\lambda$ ,  $\lambda$  and  $\tan\beta$ . This relation is generally not satisfied within the CNMSSM; then – at least for large values of  $\tan\beta$  – this mixing effect disallows values of  $\lambda \gtrsim .1$ .

When  $\lambda$  is small, the mixings between the scalar and pseudoscalar singlet and the doublet states are small and their masses read, respectively:

$$m_S^2 = \nu(A_\kappa + 4\nu), \quad m_P^2 = -3\nu A_\kappa. \quad (2.7)$$

The parameter  $A_\kappa$  being only slightly renormalized from the GUT scale down to the SUSY scale, eq. (2.7) shows that the masses of the singlet states are directly proportional to the value of  $A_\kappa$  at the GUT scale. The condition that both squared masses are positive together with eq. (2.2) implies

$$-4(B - A_\lambda)^2 \lesssim A_\kappa(B - A_\lambda) \lesssim 0. \quad (2.8)$$

The parameter  $B$ , obtained from the minimization equations (2.3) depends on  $m_0$ ,  $M_{1/2}$ ,  $\lambda$  and  $\tan\beta$ , while  $A_\lambda$  depends on  $A_0$ ,  $\lambda$  and  $\tan\beta$ . This means that, for  $\text{sign}(\mu)$  positive (which

we will always assume in the following), either  $A_\kappa > 0$  and  $A_0 > \tilde{A}_0(m_0, M_{1/2}, \lambda, \tan\beta)$  or  $A_\kappa < 0$  and  $A_0 < \tilde{A}_0(m_0, M_{1/2}, \lambda, \tan\beta)$ . Moreover, for  $A_\kappa > 0$  and  $\tan\beta$  moderate, large values of  $m_0$  or  $M_{1/2}$  (implying  $B$  large and positive) lead to a negative mass squared for the pseudoscalar singlet and are therefore disallowed. If  $\tan\beta$  is large, however,  $B$  remains small up to large values for  $m_0$  and  $M_{1/2}$  which are no longer excluded.

Finally, in the neutralino sector, we have a symmetric  $5 \times 5$  mass matrix:

$$\mathcal{M}_{\tilde{\chi}^0} = \begin{bmatrix} M_1 & 0 & \frac{g_1 h_u}{\sqrt{2}} & -\frac{g_1 h_d}{\sqrt{2}} & 0 \\ & M_2 & -\frac{g_2 h_u}{\sqrt{2}} & \frac{g_2 h_d}{\sqrt{2}} & 0 \\ & & 0 & -\mu & -\lambda h_d \\ & & & 0 & -\lambda h_u \\ & & & & 2\nu \end{bmatrix} \quad (2.9)$$

When  $\lambda \ll 1$ , the singlino decouples from other neutralinos and its mass is  $m_{\tilde{g}} = 2\nu$ . It is difficult to guess the input parameters that lead to a singlino LSP as  $\nu$  is a derived parameter. Nevertheless, using eq. (2.2) one can rewrite  $m_{\tilde{g}} = 2(B - A_\lambda)$ . One can see from eq. (2.3) that for large values of  $\tan\beta$   $B$  is small and the mass of the singlino is simply  $m_{\tilde{g}} \sim -2A_\lambda$ , i.e. it depends mainly on  $A_0$  and is insensitive to  $m_0$  and  $M_{1/2}$ . Hence, the singlino will be the LSP for large values of  $M_{1/2}$  (where the bino is heavy). For moderate values of  $\tan\beta$ , the singlino mass depends also on  $B$ , which grows like  $m_0$  and  $M_{1/2}$  and has the same sign as  $\mu$  (assumed positive). Therefore, if  $A_\kappa < 0$  and  $A_0 \lesssim \tilde{A}_0$ ,  $\nu$  is positive and a singlino LSP is likely to appear at small values of  $m_0$  and  $M_{1/2}$ . On the contrary, if  $A_\kappa > 0$  and  $A_0 \gtrsim \tilde{A}_0$ ,  $\nu$  is negative and the singlino will be the LSP at large  $m_0$  or  $M_{1/2}$ , where  $\nu \rightarrow 0$ . (We remind that in this case,  $m_0$  and  $M_{1/2}$  are bounded from above in order to have a positive mass squared for the pseudoscalar singlet).

### 3 Relic density of DM

The relic density calculation follows the usual procedure of evaluating the thermally averaged cross section for annihilation and coannihilation of the LSP and solving for the density evolution equation numerically. To do so we use **micrOMEGAS** [29] adapted for the NMSSM [22]. For this a model has been specified in the **CalcHEP** [39] format with the help of **LANHEP** [40]. Given the set of input parameters, as specified in the SLHA2 format [41, 42], the code then finds the LSP before generating with **CalcHEP** all the matrix elements of all relevant processes of annihilation and, when necessary, coannihilation. An automatic procedure for looking for s-channel poles is incorporated into the program such that a more precise integration routine can be used in the event one is close to a pole. One issue that has to be treated with special care is the one of radiative corrections to the Higgs bosons masses and couplings. Those are calculated in **NMSSMTools** and can be very important. Since knowing the precise value of the Higgs mass is often crucial to a relic density calculation, we want to use the loop-corrected masses even though **CalcHEP** computes only tree-level matrix elements. To deal with this, as was described in [22], we write a general effective potential involving two doublets and a singlet which includes 10 effective parameters. Taking the radiatively corrected Higgs masses and mixings angles provided by **NMSSMTools**, we extract the value of

these effective parameters. It is then a simple matter to derive the corresponding trilinear and quartic couplings of the scalar sector. Note however that the effective potential includes only leading operators, and that in practice the number of parameters that we can extract from observables (masses and mixings) in the Higgs sector is limited. While these operators should include the dominant corrections to the masses and vertices, this procedure can fail or show too large sensitivity to a given parameter. A signal that there might be a problem with the procedure is that one of the dimensionless effective operators is larger than 1. A warning is issued in this case <sup>2</sup>.

A complete calculation of the neutralino DM in the NMSSM defined at the weak scale has shown that often the same mechanisms as in the MSSM for neutralino annihilation are at work. In the constrained version of the models, those can be classified as

- Annihilation of a bino LSP through light sfermion exchange; this occurs at small values of  $m_0, M_{1/2}$ .
- Annihilation near a Higgs resonance (heavy or light Higgses); this requires some higgsino component. The light Higgs resonance is found for values of  $M_{1/2}$  near/below the LEP exclusion bound while the heavy Higgs resonance is found at large values of  $\tan\beta$ .
- Annihilation of a mixed bino-higgsino LSP; this occurs at very large  $m_0$  in the so-called focus point region.
- Coannihilation of a bino with sfermions; this occurs at small values of  $m_0$  when the stau is the NLSP or in a very small region at low  $m_0, M_{1/2}$  where the stop is the NLSP. The latter is possible only for large negative values of  $A_0$ .

Nevertheless in the NMSSM one finds important differences with the MSSM: the extra Higgses open up the possibility of more resonant annihilation and the singlino component of the neutralino LSP can alter the prediction for annihilation cross-sections. The new mechanism that can provide a DM candidate compatible with the WMAP results are

- Annihilation near a pseudoscalar singlet resonance, occurring at any values of  $\tan\beta$  provided  $\lambda \gtrsim .1$ .
- Coannihilation of a singlino LSP with sfermions for small values of  $m_0$  and  $\lambda \ll 1$ .
- Coannihilation of a singlino LSP with higgsino NLSP; this occurs at large  $m_0, \lambda \ll 1$  and is more likely for large values of  $\tan\beta$ .
- Coannihilation of a singlino LSP with bino NLSP, the bino rapidly annihilating through a Higgs resonance, for large  $\tan\beta$  and  $\lambda \ll 1$ .

In the following section we will give specific examples where the old and new mechanisms for LSP (co)annihilation are at work.

---

<sup>2</sup>It also means that there might be a mismatch in the Higgs to Higgs partial widths between `NMSSMTools` and `micrOMEGAs` since the set of radiative corrections to the Higgs masses that have been calculated is much more complete than the ones to the partial widths. In general the difference is  $< 10\%$ . For the purpose of computing the relic density, the Higgs to Higgs decays can play a role only near a resonance where the total width is the relevant parameter. A correction to one partial width is therefore not so crucial.

## 4 Results

We first performed a general scan over the parameter space of the CNMSSM for fixed values of the SM parameters in order to find regions satisfying all collider constraints and compatible with WMAP, that is  $\Omega h^2 < .129$ <sup>3</sup>. We quote only the upper bound since we assume that the neutralino does not necessarily account for all the DM. We used the central value of the top quark mass measured at the Tevatron,  $m_t = 171.4$  GeV [43], and choose  $m_b(m_b) = 4.214$  GeV and  $\alpha_S(M_Z) = .1172$ . Note that the top quark mass does affect the value of the light Higgs mass as well as the calculation of the spectrum at large  $m_0$  while  $m_b$  affects the Higgs masses and couplings especially at large  $\tan\beta$ . As mentioned in sec. 2, we assumed  $\text{sign}(\mu) > 0$ .

We found 2 disconnected regions in the parameter space: One at small  $\tan\beta \sim 2$  and large  $\lambda \sim .5$ , where the lightest Higgs boson is heavy enough to pass the LEP constraints due to the specific NMSSM tree level contribution to its mass as shown in eq. (2.5). The other allowed region is for small  $\lambda \lesssim .1$  and  $\tan\beta \gtrsim 4$ . In this case, the singlet sector is almost decoupled from the rest of the theory and the bound on the lightest Higgs doublet implies a lower bound on  $\tan\beta$  as in the CMSSM.

We then picked 7 couple of values for  $\lambda$  and  $\tan\beta$ :  $\lambda = .5$ ,  $\tan\beta = 2$  in the first region and  $\lambda = .1$  or  $.01$ ,  $\tan\beta = 5, 10$  or  $50$  in the second. For each couple of values of  $\lambda$ ,  $\tan\beta$  we scanned randomly on the remaining free parameters, namely  $m_0$ ,  $M_{1/2}$ ,  $A_0$ ,  $A_\kappa$ , in order to find regions in the parameter space allowed by all theoretical and experimental constraints. As mentioned in sec. 2, we found either  $A_\kappa < 0$  and  $A_0 < \tilde{A}_0(\lambda, \tan\beta)$  or  $A_\kappa > 0$  and  $A_0 > \tilde{A}_0(\lambda, \tan\beta)$ , the latter case appearing only if  $\lambda = .01$  and/or  $\tan\beta = 50$  (the other values of  $\lambda$ ,  $\tan\beta$  always lead to light states in the Higgs sector excluded by LEP when  $A_\kappa > 0$ ).

Finally, we identified the values of  $A_0$  and  $A_\kappa$  for which the main neutralino annihilation channel is a Higgs singlet resonance, or the LSP is mainly singlino. For the former case we found either  $\lambda = .5$ ,  $\tan\beta = 2$  and  $A_0 \sim A_\kappa$  large and negative, or  $\lambda = .1$ , large  $A_0 < 0$  and small  $A_\kappa < 0$ . For  $\lambda = .1$ ,  $\tan\beta = 50$  we also found singlet resonances at large  $A_0 > 0$  and small  $A_\kappa > 0$ . The singlino LSP scenario on the other hand appears only for  $\lambda = .01$ . It requires  $A_\kappa < 0$  and  $A_0 \lesssim \tilde{A}_0(\tan\beta)$  or  $A_\kappa > 0$  and  $A_0 \gtrsim \tilde{A}_0(\tan\beta)$ . We will now present plots in the  $m_0, M_{1/2}$  plane for selected values of  $\lambda$ ,  $\tan\beta$ ,  $A_0$  and  $A_\kappa$ .

### 4.1 Large $\lambda$ : singlet resonances

We first consider the cases where  $\lambda = .5$  or  $.1$ . Here, the LSP is mainly bino and is not expected to have a large singlino component. The constraints from Higgs searches at LEP can be very important, especially at small values of  $\tan\beta$ , when considering the rather low value of the top quark mass now measured at Fermilab,  $m_t = 171.4$  GeV.

---

<sup>3</sup>The most recent WMAP and SDSS results give tighter constraints on the relic density of DM [44, 45]. However adopting a more conservative approach when fitting this data, that is allowing extra degrees of freedom in the cosmological model used [46], leads to the range  $.094 < \Omega h^2 < .136$  [47], giving results similar to the ones we discuss below.

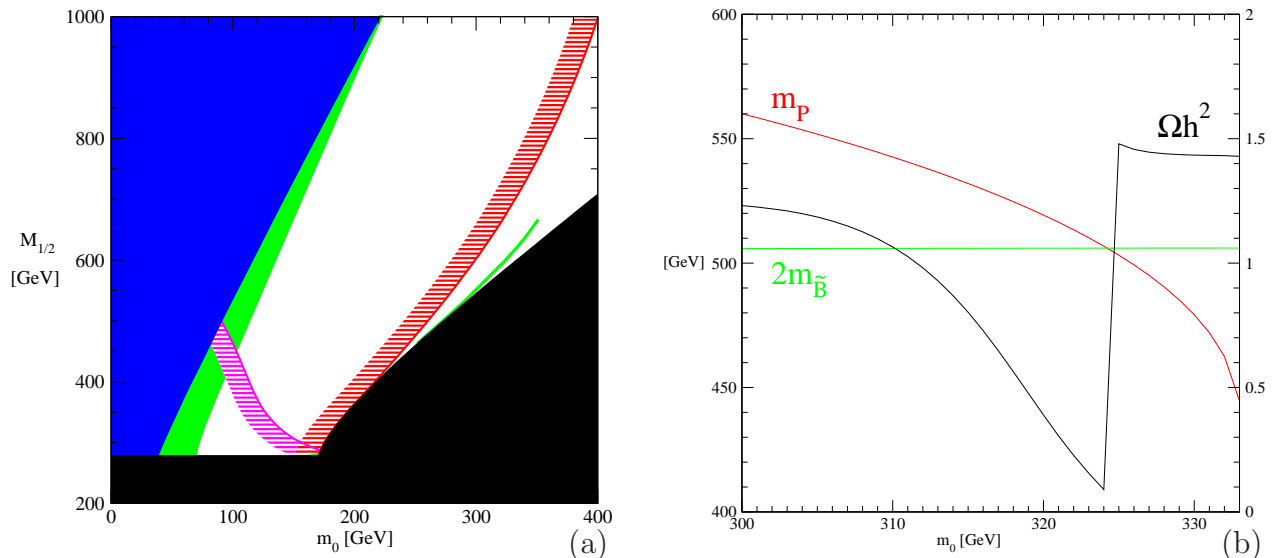


Figure 1: (a) The WMAP allowed region (green) in the  $m_0, M_{1/2}$  plane for  $\lambda = .5$ ,  $\tan\beta = 2$ ,  $A_0 = -1300$  GeV,  $A_\kappa = -1400$  GeV. We show the region excluded by theoretical constraints or by LEP searches on sparticles (black), the region where a sfermion – the lightest stau here – is the LSP (blue), the LEP limit from Higgs searches (red/hatch) and the contour  $m_h = 111$  GeV (pink/hatch). (b) The DM relic density  $\Omega h^2$  (black), the pseudoscalar singlet mass  $m_P$  (red) and twice the bino LSP mass  $m_{\tilde{B}}$ , as a function of  $m_0$  for the same choice of parameters and  $M_{1/2} = 600$  GeV.

#### 4.1.1 Small $\tan\beta$

The case  $\tan\beta = 2$  is very characteristic of the NMSSM. Indeed, when  $\lambda$  is near its maximal value and  $\tan\beta$  is small, the light Higgs doublet can be heavier than in the MSSM, as already mentioned, so it is possible to satisfy the LEP constraints. Nevertheless, for  $\tan\beta = 2$  and  $\lambda = .5$ , large regions of parameter space are excluded by experimental or theoretical constraints. For large negative values of  $A_\kappa$  and  $A_0$ , however, one finds allowed regions in the parameter space with the right order of magnitude for the relic density of DM. In some cases, the main neutralino annihilation channel is a pseudoscalar singlet resonance. We show in fig. 1(a) the various constraints in the  $m_0, M_{1/2}$  plane for  $A_0 = -1300$  GeV and  $A_\kappa = -1400$  GeV. The large  $m_0$  region is theoretically excluded as well as the region  $M_{1/2} \lesssim 280$  GeV. Along the region where the lightest stau is the LSP, at small  $m_0$ , one finds a broad band where the DM relic density is below the WMAP upper bound. In this band, the bino LSP coannihilates with the stau (as in the CMSSM). Applying strictly the LEP limits on Higgs searches from each decay channel, as it is done in `NMSSMTools`, excludes a large fraction of the parameter space, including this WMAP compatible band. Note however that allowing for some theoretical uncertainty in the Higgs mass calculation (estimated to be  $\sim 3$  GeV) would restore most of the forbidden parameter space. In particular, most of the WMAP compatible bino-stau coannihilation region has  $m_h > 111$  GeV. In the narrow region allowed by both theoretical and collider constraints, one finds a thin band allowed by WMAP where the bino LSP rapidly annihilates through a pseudoscalar singlet resonance. In fig. 1(b) we show DM relic density, the pseudoscalar singlet mass and twice the bino LSP mass as a function of  $m_0$  for the same choice of parameters as fig. 1(a) and  $M_{1/2} = 600$  GeV.

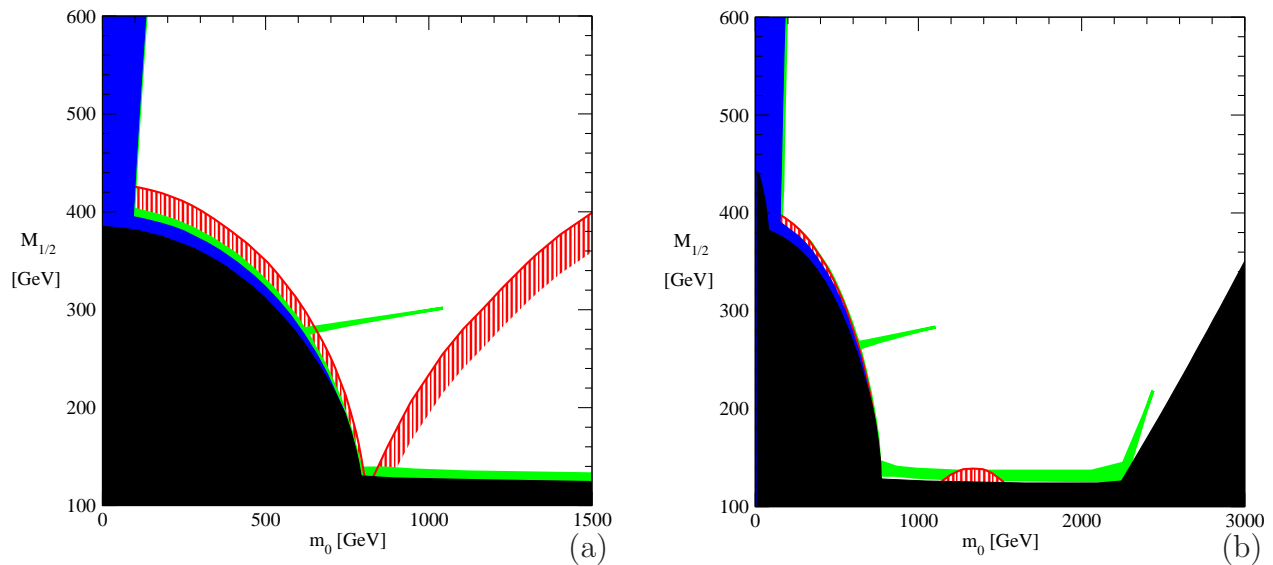


Figure 2: The WMAP allowed region in the  $m_0, M_{1/2}$  plane for (a)  $\lambda = .1$ ,  $\tan\beta = 5$ ,  $A_0 = -1500$  GeV,  $A_\kappa = -50$  GeV and (b)  $\lambda = .1$ ,  $\tan\beta = 10$ ,  $A_0 = -1500$  GeV,  $A_\kappa = -50$  GeV. Same color code as in fig. 1

#### 4.1.2 Intermediate $\tan\beta$

As explained in sec. 2, increasing  $\tan\beta$  implies  $\lambda \lesssim .1$ , larger values leading to a light scalar Higgs doublet excluded by LEP. We took  $\lambda = .1$ ,  $\tan\beta = 5$  or 10 and found that large  $A_0 < 0$ , small  $A_\kappa < 0$  are favorable for bino LSP annihilation through a Higgs resonance. The possible resonances are the pseudoscalar singlet  $P$  or the lightest scalar doublet  $h$ . As an example we consider  $A_0 = -1500$  GeV,  $A_\kappa = -50$  GeV, see fig. 2.

The possibility of annihilation through a pseudoscalar resonance at intermediate values of  $\tan\beta$  is a characteristic feature of the NMSSM. In our case study, the pseudoscalar singlet resonance is found around  $M_{1/2} \sim 300$  GeV, and corresponds to  $|2m_{\tilde{B}} - m_P| \lesssim 3$  GeV. For larger negative values of  $A_\kappa$ ,  $m_P$  increases, as can be seen from eq. (2.7), which means that rapid annihilation would be possible for a heavier bino LSP, that is a larger  $M_{1/2}$ . However, when  $m_{\tilde{B}}$  is large it becomes increasingly difficult to rely exclusively on Higgs exchange to have efficient enough annihilation. Thus, for large negative values of  $A_\kappa$ , the rapid annihilation region disappears. The pseudoscalar singlet exchange is also dominant in the small region compatible with WMAP around  $m_0 \sim 2.3$  TeV, see fig. 2(b). When annihilation is dominated by the pseudoscalar singlet exchange, the annihilation channels are purely into  $b\bar{b}$  and  $\tau\tau$  pairs for light pseudoscalars, whereas the  $t\bar{t}$  channel can contribute significantly, once passed the top threshold.

Rapid annihilation of the bino LSP through the light scalar doublet  $h$  can also occur at low values of  $M_{1/2} \sim 130$  GeV. Note however that, as in the CMSSM, the small  $M_{1/2}$  region is constrained by chargino searches and Higgs searches at LEP, especially at small  $\tan\beta$ . For  $\tan\beta = 5$ , the Higgs constraint rules out practically all the scalar doublet annihilation region. For  $\tan\beta = 10$ , the Higgs bound is relaxed and, both the WMAP and the Higgs constraints are satisfied for  $M_{1/2} \sim 130$  GeV except in a window  $1.1 \lesssim m_0 \lesssim 1.5$  TeV. Alternatively, one could have increased  $|A_0|$  to relax the Higgs bound.

Sfermion coannihilation can also provide a mechanism to lower the relic density below

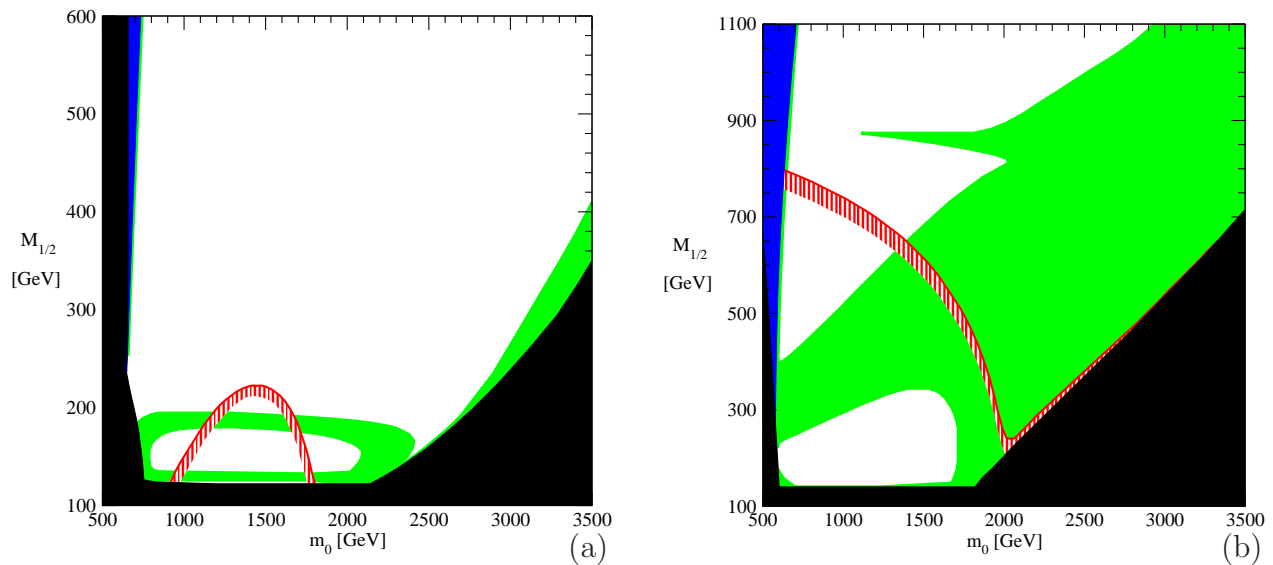


Figure 3: The WMAP allowed region in the  $m_0, M_{1/2}$  plane for (a)  $\lambda = .1$ ,  $\tan\beta = 50$ ,  $A_0 = -1500$  GeV,  $A_\kappa = -50$  GeV and (b)  $\lambda = .1$ ,  $\tan\beta = 50$ ,  $A_0 = 1500$  GeV,  $A_\kappa = 250$  GeV. Same color code as in fig. 1

the WMAP upper bound. As in the MSSM, we find a stau coannihilation band for values of  $m_0$  just above the stau LSP forbidden region as well as a narrow stop coannihilation region at small values of  $m_0$  and  $M_{1/2}$  just above the stop LSP forbidden region. Note that the latter can only be found for large negative values of  $A_0$  and it satisfies the LEP constraints on the Higgs sector only when  $\tan\beta = 10$ . Smaller values of  $m_0, M_{1/2}$  are excluded as they lead to a negative squared mass in the stop sector.

#### 4.1.3 Large $\tan\beta$

We next consider the case  $\tan\beta = 50$ ,  $\lambda = .1$ . First note that one can find WMAP compatible regions for  $A_0, A_\kappa < 0$ , as we had for intermediate values of  $\tan\beta$ , but also for  $A_0, A_\kappa > 0$ . In the former case, DM annihilation mechanisms are sfermion coannihilation and Higgs exchange annihilation. This is illustrated in fig. 3(a) for  $A_0 = -1500$  GeV,  $A_\kappa = -50$  GeV. The possible Higgs resonances are again the light scalar doublet  $h$  at low  $M_{1/2} \sim 130$  GeV, just above the chargino exclusion limit from LEP, or the pseudoscalar singlet  $P$  for slightly larger values of  $M_{1/2} \sim 200$  GeV. For  $2 \lesssim m_0 \lesssim 2.5$  TeV and  $130 \lesssim M_{1/2} \lesssim 200$  GeV one also finds a WMAP allowed band where the bino LSP rapidly annihilates through the pseudoscalar singlet resonance. The special features of the region  $m_0 \gtrsim 2.5$  TeV will be discussed in the next subsection. The LEP constraints on the Higgs sector excludes the region at small  $M_{1/2}$  where  $.9 \lesssim m_0 \lesssim 1.8$  TeV. For  $m_0 \sim 750$  GeV and  $130 \lesssim M_{1/2} \lesssim 200$  GeV, the bino LSP coannihilates with the stop NLSP. For larger values of  $M_{1/2}$ , one also finds a bino-stau coannihilation thin band along the forbidden stau LSP region. Smaller values of  $m_0 \lesssim 750$  GeV are excluded as they would lead to negative sfermion masses.

When  $A_0$  and  $A_\kappa$  are both positive, all Higgs states, except the scalar singlet  $S$ , can be light and contribute significantly to the bino LSP annihilation. In fig. 3(b), we consider  $A_0 = 1500$  GeV and  $A_\kappa = 250$  GeV. First we focus on the region  $m_0 \lesssim 2.5$  TeV. Larger values of  $m_0$  will be treated in the next subsection. The WMAP compatible regions correspond

to the resonances of the light scalar doublet  $h$  just above the chargino exclusion limit from LEP at  $M_{1/2} \sim 130$  GeV, of the heavy scalar/pseudoscalar doublets  $H/A$  in a wide band for  $130 \lesssim M_{1/2} \lesssim 800$  GeV, and of the pseudoscalar singlet  $P$  at still larger values of  $M_{1/2} \sim 900$  GeV. Note however that the regions around the lighter resonances are ruled out by the LEP limit on the Higgs sector. The annihilation channels near the  $P$  resonance are into  $b\bar{b}$ ,  $\tau\tau$ , as well as  $WH^\pm$ ,  $hA$  or  $ZH$ . Of course coannihilation with sfermions is always possible when  $m_0$  is near its lower bound.

#### 4.1.4 Large $m_0$

In the CMSSM, the interest from the point of view of compatibility with WMAP of the large  $m_0$  region has been widely stressed. The main reason is that the parameter  $\mu$  decreases sharply as  $m_0$  increases, before entering an unphysical region where  $\mu^2 < 0$ . When  $\mu < M_1$ , the LSP has an important higgsino component and can annihilate efficiently into  $W$  pairs.

In the CNMSSM,  $\mu$  also decreases at large  $m_0$ , although one needs to take into account another factor: the squared mass of the lightest pseudoscalar Higgs state can become negative at large  $m_0$ , thus leading to an unphysical region before the higgsino becomes LSP. This is precisely what happens in the example we have considered previously with  $\tan\beta = 10$ , in fig. 2(b). Large values of  $m_0$  are excluded as they would lead to a negative mass squared in the Higgs sector and the higgsino component of the LSP remains well below 10% over the parameter space of the theoretically allowed region, so the annihilation into  $W$  pairs is not efficient and the relic density is too large.

For  $\tan\beta = 50$  and  $A_\kappa < 0$ , as displayed in fig. 3(a), the higgsino component of the LSP is also small over the allowed parameter space at  $m_0 \gtrsim 2.5$  TeV. On the other hand annihilation through the heavy Higgs doublet  $H/A$  exchange is efficient, especially considering the  $\tan\beta$  enhanced couplings to  $b\bar{b}$  and  $\tau\tau$ . This leads to an allowed band at large  $m_0$  along the boundary of the theoretically excluded region. Note that there is a very narrow region at this boundary, hardly distinguishable given the scale of the figure, where the lightest pseudoscalar is excluded by LEP, just before its mass squared becomes negative.

Finally, in the case  $\tan\beta = 50$ ,  $A_\kappa > 0$ , fig. 3(b), the higgsino component of the LSP can be large at  $m_0 \gtrsim 2.5$  TeV near the theoretically excluded region, i.e. in the lower part of the wide WMAP allowed band. In this region, the annihilation channels are typical of a higgsino LSP:  $WW$ ,  $b\bar{b}$  as well as coannihilation channels with the charginos or with heavier neutralinos. In the upper part of the wide WMAP allowed band at large  $m_0$ , annihilation is dominated by the exchange of the heavy scalar/pseudoscalar doublet  $H/A$ , as well as the pseudoscalar singlet  $P$ . The annihilation products include a variety of channels such as  $b\bar{b}$ ,  $\tau\tau$ ,  $WH^\pm$ ,  $hA$  or  $ZH$ . Note that in fig. 3(b) it is possible to distinguish the thin region where the lightest pseudoscalar is excluded by LEP above the theoretically excluded region where its mass squared becomes negative.

## 4.2 Small $\lambda$ : singlino LSP

Next we focus on the regions of parameter space where a singlino LSP can be found. As already mentioned, this scenario appears only for  $\lambda = .01$  in our selected scans. Qualitatively the results are similar for smaller values of  $\lambda$ . In this case, we have an effective MSSM with an almost decoupled singlet sector and we do not expect to have singlet Higgs resonances.

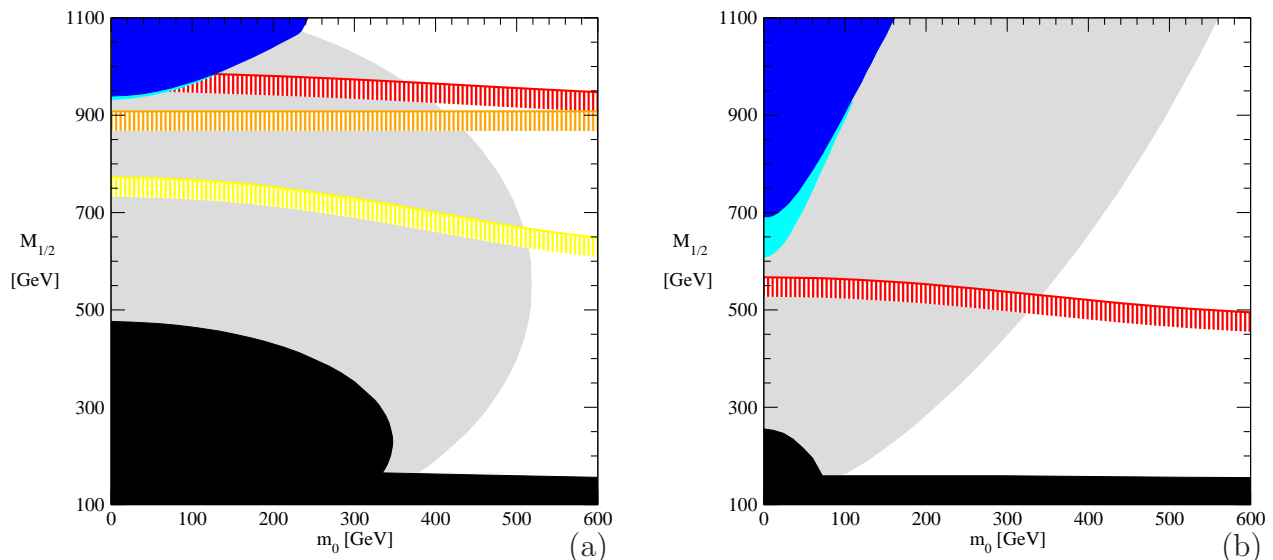


Figure 4: The WMAP allowed region in the  $m_0, M_{1/2}$  plane (cyan) for (a)  $\lambda = .01, \tan\beta = 5, A_0 = 200$  GeV,  $A_\kappa = -10$  GeV and (b)  $\lambda = .01, \tan\beta = 10, A_0 = -20$  GeV,  $A_\kappa = -50$  GeV. We show the region excluded by theoretical constraints or by LEP searches on sparticles (black), the region where the stau is the LSP (blue), the region where the singlino is the LSP (grey), the LEP exclusion on the Higgs sector (red/hatch). In (a) we also show the LEP constraint on the Higgs sector for  $\lambda = .001$  (orange/hatch) or  $m_t = 175$  GeV (yellow/hatch).

#### 4.2.1 Intermediate $\tan\beta$

While scanning over  $A_0, A_\kappa, m_0, M_{1/2}$  with  $\lambda = .01$  and  $\tan\beta = 5$  or  $10$ , we have not found regions where rapid annihilation through a Higgs exchange could take place. Thus the only mechanism that can provide the correct relic density for a singlino LSP is coannihilation with a slepton NLSP. This works most efficiently when the LSP and NLSP are well below the TeV scale. We therefore expect to find WMAP allowed regions for choices of input parameters that predict a singlino LSP at low values of  $m_0$  and  $M_{1/2} \lesssim 1$  TeV. This means that  $A_0$  cannot be too large, cf. sec. 2.

Let us start with  $A_\kappa < 0$ . As explained in sec. 2, in this case the singlino mass  $m_{\tilde{g}} = 2\nu$  is positive and grows with  $m_0$  and  $M_{1/2}$ . Therefore, one expects to find a singlino LSP for small values of the soft masses. For  $\tan\beta = 5, A_0 = 200$  GeV,  $A_\kappa = -10$  GeV, fig. 4(a), the singlino is the LSP for  $m_0 \lesssim 500$  GeV,  $M_{1/2} \lesssim 1100$  GeV. Most of the singlino LSP region is excluded by the LEP constraints on the Higgs. The singlino LSP satisfies the WMAP upper limit in a narrow band just below the stau LSP excluded region. There, the singlino LSP, which mass is  $m_{\tilde{g}} \sim 350 - 380$  GeV, coannihilates with the stau and other sleptons. The entire WMAP compatible area where the LSP is a singlino can however escape the LEP constraints for smaller values of  $\lambda$  (e.g.  $\lambda = .001$ ) or for a larger top quark mass (e.g.  $m_t = 175$  GeV). Increasing  $\tan\beta = 10$  also reduces the impact of the LEP constraint on the Higgs mass. For example, assuming  $A_0 = -20$  GeV,  $A_\kappa = -50$  GeV one finds a WMAP compatible singlino LSP region just below the area at low  $m_0$  where the stau is the LSP, see fig. 4(b).

For  $A_\kappa > 0$ , the singlino mass still grows with  $m_0$  and  $M_{1/2}$  but is negative. Therefore, the singlino LSP is rather found at large values of  $m_0, M_{1/2}$ , just below the excluded region

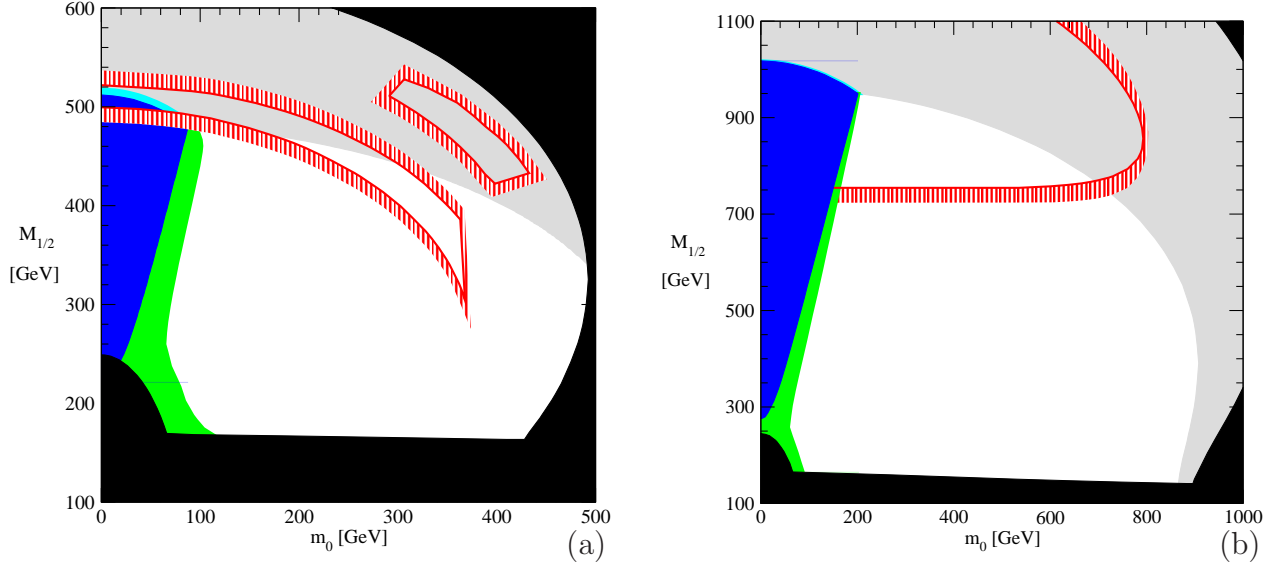


Figure 5: The WMAP allowed region in the  $m_0, M_{1/2}$  plane (green for bino LSP, cyan for singlino LSP) for (a)  $\lambda = .01$ ,  $\tan\beta = 10$ ,  $A_0 = 250$  GeV,  $A_\kappa = 270$  GeV and (b)  $\lambda = .01$ ,  $\tan\beta = 5$ ,  $A_0 = 750$  GeV,  $A_\kappa = 10$  GeV (here  $m_t = 175$  GeV). Same color code as fig. 4.

where the pseudoscalar singlet mass squared becomes negative. However, these choices of parameters always lead to light states in the Higgs sector, excluded by LEP. Yet for  $\tan\beta = 10$ ,  $A_0 = 250$  GeV,  $A_\kappa = 270$  GeV, one still finds a region where singlino-stau coannihilation is just enough to satisfy the WMAP bound while LEP constraints on the Higgs are satisfied, see fig. 5(a). For  $\tan\beta = 5$  it is difficult to find a WMAP compatible region not excluded by LEP constraints. However assuming  $m_t = 175$  GeV, one can find such an allowed region see fig. 5(b). In all cases, the mass difference between the singlino and the stau must be  $\lesssim 3$  GeV for the coannihilation mechanism to be efficient enough.

#### 4.2.2 Large $\tan\beta$

For  $\tan\beta = 50$ , the singlino mass depends mainly on  $A_0$ , as discussed in sec. 2. Hence, for large values of  $M_{1/2}$  the bino is heavy and the singlino can be the LSP. One also expects more Higgs resonances as for  $\lambda = .1$ ,  $\tan\beta = 50$  above, or in the CMSSM at large  $\tan\beta$ .

Let us start with the case  $A_0 = -1000$  GeV,  $A_\kappa = -50$  GeV, as illustrated in fig. 6(a). For  $M_{1/2} \lesssim 1.4$  TeV, the situation is similar to the CMSSM: the LSP is mainly bino and its relic density is below the WMAP upper bound either if it coannihilates with the stau NLSP at low values of  $m_0$  (close to the forbidden zone where the stau is the LSP) or if it annihilates rapidly through a Higgs resonance. The light Higgs doublet  $h$  can play this role near  $M_{1/2} \sim 130$  GeV, although this area is mostly excluded by the LEP constraints on the Higgs sector. The heavy scalar/pseudoscalar doublet  $H/A$  can also play this role either for  $m_0 \sim 1$  TeV,  $M_{1/2} \sim 1.3$  TeV or at large  $m_0$ , above the excluded region where the lightest pseudoscalar mass squared becomes negative. When one approaches this theoretically excluded region at very large values of  $m_0 \gtrsim 4$  TeV, the higgsino component of the LSP increases and its relic density drops due to rapid annihilation into  $W$  pairs and coannihilation with charginos or heavier neutralinos. For  $M_{1/2} \lesssim 1.4$  TeV, the only difference with the CMSSM is the small WMAP compatible zone at  $m_0 \sim 2.2$  TeV,  $M_{1/2} \sim 260$  GeV where the bino LSP rapidly

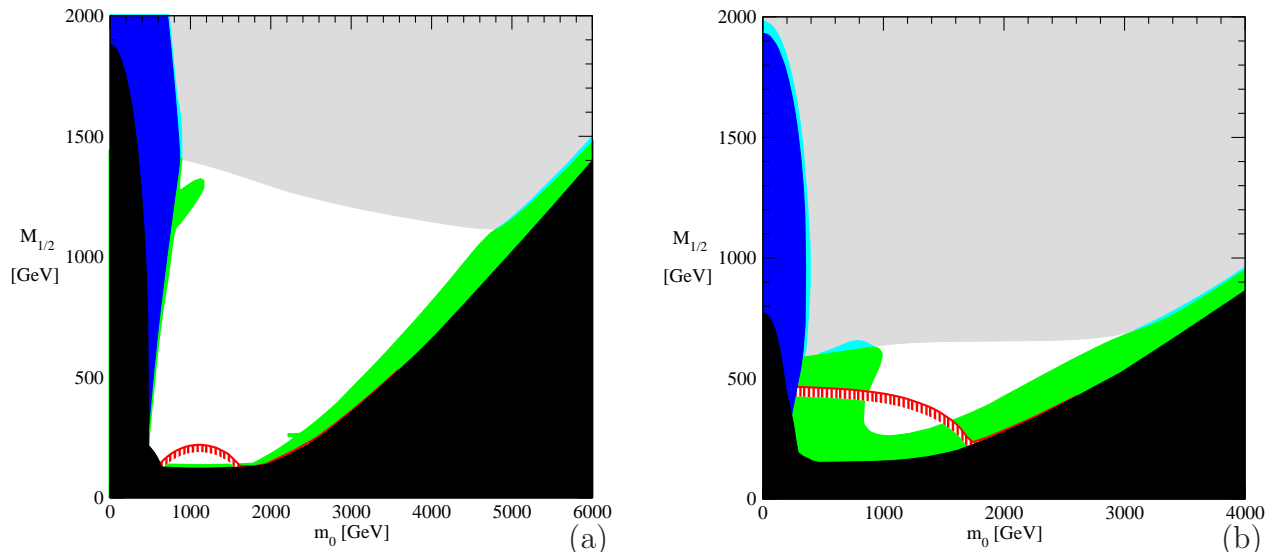


Figure 6: The WMAP allowed region in the  $m_0$ ,  $M_{1/2}$  plane for (a)  $\lambda = .01$ ,  $\tan\beta = 50$ ,  $A_0 = -1000$  GeV,  $A_\kappa = -50$  GeV and (b)  $\lambda = .01$ ,  $\tan\beta = 50$ ,  $A_0 = 0$  GeV,  $A_\kappa = 50$  GeV. Same color code as fig. 5.

annihilates through resonance of the pseudoscalar singlet  $P$ . When  $M_{1/2} \gtrsim 1.4$  TeV, the LSP is mainly singlino and its relic density is below the WMAP upper bound either if it coannihilates with the stau NLSP at low values of  $m_0$  or if it coannihilates with the mixed bino-higgsino NLSP at very large values of  $m_0 \gtrsim 5$  TeV. Note that the WMAP compatible singlino LSP region at large  $m_0$  does not extend all the way to the theoretically excluded region: indeed, as  $m_0$  increases,  $\mu$  decreases and the LSP becomes predominantly higgsino.

For  $A_\kappa > 0$  the situation is similar. In fig. 6(b) we display our results for  $A_0 = 0$ ,  $A_\kappa = 50$  GeV. Now the singlino is the LSP for  $M_{1/2} \gtrsim 600$  GeV and its relic density is below the WMAP upper bound in 3 different regions: At low  $m_0$  where it coannihilates with the stau NLSP. For  $M_{1/2} \sim 600$  GeV and  $400 \text{ GeV} \lesssim m_0 \lesssim 1000$  GeV, where it coannihilates with the bino NLSP which in turn annihilates rapidly through the heavy scalar/pseudoscalar doublet  $H/A$  resonance. Finally, at large  $m_0$  the singlino LSP coannihilates with the mixed bino-higgsino NLSP, which in turn annihilates rapidly through the  $H/A$  resonance or into typical higgsino channels, including  $W$  pairs or coannihilation with charginos and heavier neutralinos. Here again, the WMAP compatible singlino LSP region does not extend all the way to the theoretically excluded region but stops where the LSP becomes mainly higgsino.

## 5 Discussion

We have achieved a first exploration of the parameter space of the CNMSSM from the point of view of DM relic density, taking into account all theoretical and collider constraints. We have presented our results in the  $m_0$ ,  $M_{1/2}$  plane for selected values of  $\lambda$ ,  $\tan\beta$ ,  $A_0$  and  $A_\kappa$ . We have assumed  $\text{sign}(\mu) > 0$ , yet we do not expect any change in our analysis for  $\text{sign}(\mu) < 0$ . We have recovered the main scenarios of the MSSM as well as new ones. For  $\lambda \gtrsim .1$  we have shown that it was possible to have an extra pseudoscalar singlet resonance at any values of  $\tan\beta$ . The search of this extra Higgs state might reveal an interesting challenge

at LHC [48]. Although this pseudoscalar singlet state is not very heavy its couplings to fermions are suppressed relative to a doublet pseudoscalar making the pseudoscalar invisible unless  $\tan\beta$  is large [49]. For small  $\lambda = .01$ , we have shown that it was possible to have a singlino LSP with a relic density below the WMAP upper bound. However, such scenarios always require coannihilation with the stau, bino or mixed bino-higgsino NLSP, and a small mass difference between the singlino LSP and the NLSP ( $\lesssim 3$  GeV). In these coannihilation scenarios, the presence of a singlino LSP in the decay of the NLSP (sfermion or neutralino) might influence markedly the phenomenology at colliders [50, 51]. The consequences for indirect detection of dark matter in all the WMAP compatible scenarios will be analysed in a separate publication [52]. These scenarios represent only a subset of the possible scenarios for the singlino LSP DM in the general NMSSM. Indeed, in the model with free parameters at the weak scale, it is also possible to have annihilation of singlino LSP through a Z or a light scalar/pseudoscalar resonance or to have annihilation of a mixed singlino-higgsino LSP into  $W$  or Higgs pairs. Such scenarios usually require  $\lambda \gtrsim .1$  while  $\nu < \mu$ . In the CNMSSM, both  $\mu$  and  $\nu$  are derived quantity, and such scenarios are absent.

## Acknowledgments

We would like to thank U. Ellwanger, F. Boudjema and Y. Mambrini for helpful discussions. This work was supported in part by GDRI-ACPP of CNRS.

## References

- [1] D. N. Spergel *et al.* [WMAP Collaboration], *Astrophys. J. Suppl.* **148** (2003) 175 [arXiv:astro-ph/0302209].
- [2] J. R. Ellis, K. A. Olive, Y. Santoso and V. C. Spanos, *Phys. Lett. B* **565** (2003) 176 [arXiv:hep-ph/0303043].
- [3] H. Baer and C. Balazs, *JCAP* **0305** (2003) 006 [arXiv:hep-ph/0303114].
- [4] U. Chattopadhyay, A. Corsetti and P. Nath, *Phys. Rev. D* **68**, 035005 (2003) [arXiv:hep-ph/0303201].
- [5] S. Profumo and C. E. Yaguna, *Phys. Rev. D* **70**, 095004 (2004) [arXiv:hep-ph/0407036].
- [6] E. A. Baltz and P. Gondolo, *JHEP* **0410**, 052 (2004) [arXiv:hep-ph/0407039].
- [7] B. C. Allanach, C. G. Lester and A. M. Weber, *JHEP* **0612**, 065 (2006) [arXiv:hep-ph/0609295].
- [8] L. Roszkowski, R. Ruiz de Austri and R. Trotta, arXiv:hep-ph/0705.2012.
- [9] J. Ellis, S. Heinemeyer, K. A. Olive, A. M. Weber and G. Weiglein, arXiv:hep-ph/0706.0652.
- [10] H. P. Nilles, M. Srednicki and D. Wyler, *Phys. Lett. B* **124** (1983) 337.

- [11] J. M. Frere, D. R. T. Jones and S. Raby, Nucl. Phys. B **222**, 11 (1983).
- [12] J. P. Derendinger and C. A. Savoy, Nucl. Phys. B **237**, 307 (1984).
- [13] J. R. Ellis, J. F. Gunion, H. E. Haber, L. Roszkowski and F. Zwirner, Phys. Rev. D **39**, 844 (1989).
- [14] M. Drees, Int. J. Mod. Phys. A **4**, 3635 (1989).
- [15] U. Ellwanger, M. Rausch de Traubenberg and C. A. Savoy, Phys. Lett. B **315**, 331 (1993) [arXiv:hep-ph/9307322].
- [16] U. Ellwanger, M. Rausch de Traubenberg and C. A. Savoy, Nucl. Phys. B **492**, 21 (1997) [arXiv:hep-ph/9611251].
- [17] S. F. King and P. L. White, Phys. Rev. D **52**, 4183 (1995) [arXiv:hep-ph/9505326].
- [18] F. Franke and H. Fraas, Int. J. Mod. Phys. A **12**, 479 (1997) [arXiv:hep-ph/9512366].
- [19] R. Flores, K. A. Olive and D. Thomas, Phys. Lett. B **245** (1990) 509.
- [20] A. Stephan, Phys. Lett. B **411** (1997) 97 [arXiv:hep-ph/9704232].
- [21] A. Stephan, Phys. Rev. D **58** (1998) 035011 [arXiv:hep-ph/9709262].
- [22] G. Belanger, F. Boudjema, C. Hugonie, A. Pukhov and A. Semenov, JCAP **0509**, 001 (2005) [arXiv:hep-ph/0505142].
- [23] J. F. Gunion, D. Hooper and B. McElrath, Phys. Rev. D **73**, 015011 (2006) [arXiv:hep-ph/0509024].
- [24] D. G. Cerdeno, E. Gabrielli, D. E. Lopez-Fogliani, C. Munoz and A. M. Teixeira, arXiv:hep-ph/0701271.
- [25] R. A. Flores, K. A. Olive and D. Thomas, Phys. Lett. B **263** (1991) 425.
- [26] D. G. Cerdeno, C. Hugonie, D. E. Lopez-Fogliani, C. Munoz and A. M. Teixeira, JHEP **0412** (2004) 048 [arXiv:hep-ph/0408102].
- [27] F. Ferrer, L. M. Krauss and S. Profumo, Phys. Rev. D **74** (2006) 115007 [arXiv:hep-ph/0609257].
- [28] U. Ellwanger and C. Hugonie, arXiv:hep-ph/0612134.
- [29] G. Belanger, F. Boudjema, A. Pukhov and A. Semenov, Comput. Phys. Commun. **176**, 367 (2007) [arXiv:hep-ph/0607059].
- [30] C. Panagiotakopoulos and K. Tamvakis, Phys. Lett. B **469**, 145 (1999) [arXiv:hep-ph/9908351].
- [31] C. Panagiotakopoulos and A. Pilaftsis, Phys. Rev. D **63**, 055003 (2001) [arXiv:hep-ph/0008268].

- [32] A. Dedes, C. Hugonie, S. Moretti and K. Tamvakis, Phys. Rev. D **63**, 055009 (2001) [arXiv:hep-ph/0009125].
- [33] C. Hugonie, J. C. Romao and A. M. Teixeira, JHEP **0306** (2003) 020 [arXiv:hep-ph/0304116].
- [34] A. Menon, D. E. Morrissey and C. E. M. Wagner, Phys. Rev. D **70**, 035005 (2004) [arXiv:hep-ph/0404184].
- [35] S. J. Huber, T. Konstandin, T. Prokopec and M. G. Schmidt, Nucl. Phys. B **757**, 172 (2006) [arXiv:hep-ph/0606298].
- [36] C. Balazs, M. Carena, A. Freitas and C. E. M. Wagner, arXiv:hep-ph/0705.0431.
- [37] U. Ellwanger, J. F. Gunion and C. Hugonie, JHEP **0502**, 066 (2005) [arXiv:hep-ph/0406215].
- [38] U. Ellwanger and C. Hugonie, arXiv:hep-ph/0612133.
- [39] A. Pukhov, arXiv:hep-ph/0412191.
- [40] A. V. Semenov, arXiv:hep-ph/0208011.
- [41] P. Skands *et al.*, JHEP **0407**, 036 (2004) [arXiv:hep-ph/0311123].
- [42] B. C. Allanach *et al.*, arXiv:hep-ph/0602198;
- [43] E. Brubaker *et al.* [Tevatron Electroweak Working Group], arXiv:hep-ex/0608032.
- [44] M. Tegmark *et al.*, Phys. Rev. D **74** (2006) 123507 [arXiv:astro-ph/0608632].
- [45] D. N. Spergel *et al.* [WMAP Collaboration], arXiv:astro-ph/0603449.
- [46] O. Lahav and A. R. Liddle, arXiv:astro-ph/0601168.
- [47] J. Hamann, S. Hannestad, M. S. Sloth and Y. Y. Y. Wong, Phys. Rev. D **75**, 023522 (2007) [arXiv:astro-ph/0611582].
- [48] U. Ellwanger, J. F. Gunion and C. Hugonie, JHEP **0507**, 041 (2005) [arXiv:hep-ph/0503203].
- [49] G. Bélanger, C. Hugonie, A. Pukhov, Contributed to *Physics at TeV colliders*, Les Houches (2007).
- [50] U. Ellwanger and C. Hugonie, Eur. Phys. J. C **5** (1998) 723 [arXiv:hep-ph/9712300].
- [51] S. Kraml and W. Porod, Phys. Lett. B **626** (2005) 175 [arXiv:hep-ph/0507055].
- [52] C. Hugonie, Y. Mambrini, E. Nezri, A. Pukhov, in preparation.